

# Improving the extensional rheological properties and foamability of high-density polyethylene by means of chemical crosslinking

Ester Laguna-Gutierrez<sup>1</sup>, Javier Pinto<sup>1,2</sup>, Vipin Kumar<sup>3</sup>, Maria L Rodriguez-Mendez<sup>4</sup> and Miguel A Rodriguez-Perez<sup>1</sup>

Journal of Cellular Plastics

0(0) 1–25

© The Author(s) 2016

Reprints and permissions:

sagepub.co.uk/journalsPermissions.nav

DOI: 10.1177/0021955X16681454

cel.sagepub.com



## Abstract

Obtaining high-density polyethylene-based microcellular foams is a topic of interest due to the synergistic properties that can be obtained by the fact of achieving a microcellular structure using a polymer with a high number of interesting properties. However, due to the high crystallinity of this polymer, the production of low-density microcellular foams, by a physical foaming process, is not a simple task. In this work, the proposed solution to produce these materials is based on using crosslinked high-density polyethylenes. By crosslinking the polymer matrix, it is possible to increase the amount of gas available for foaming and also to improve the extensional rheological properties. In addition, the foaming time and the foaming temperature have also been modified with the aim of analyzing and understanding the mechanisms taking place during the foaming process to finally obtain cellular materials with low densities and improved cellular structures. The results indicate that cellular materials with relative densities of 0.37 and with cell sizes of approximately  $2\ \mu\text{m}$  can be produced from crosslinked

<sup>1</sup>Cellular Materials Laboratory (CellMat), Condensed Matter Physics Department, University of Valladolid, Valladolid, Spain

<sup>2</sup>Nanophysics-Smart Materials Group, Istituto Italiano di Tecnologia (IIT), Genova, Italy

<sup>3</sup>Department of Mechanical Engineering, University of Washington, Seattle, WA USA

<sup>4</sup>Department of Inorganic Chemistry, Industrial Engineers School, University of Valladolid, Valladolid, Spain

## Corresponding author:

Ester Laguna-Gutierrez, Cellular Materials Laboratory (CellMat), Condensed Matter Physics Department, University of Valladolid, Paseo de Belen, 7, 47011 Valladolid, Spain.

Email: ester.laguna@fmc.uva.es

high-density polyethylene using the appropriate crosslinking degree and foaming parameters.

### **Keywords**

Crosslinked foams, physical foaming, cell growth, foam density, solubility, thermoplastic foams, extensional rheology

## **Introduction**

Microcellular foams are characterized by having average cell sizes in the order of 10  $\mu\text{m}$  and cell densities higher than  $10^9$  cells  $\text{cm}^{-3}$ .<sup>1</sup> The concept of microcellular materials was created in the earlier 1980s in response to food and packaging companies to reduce materials cost without compromising mechanical properties.<sup>2</sup> These microcellular foams exhibit higher Charpy impact strength and toughness as well as higher fatigue life and thermal stability than conventional cellular materials.<sup>1</sup>

One of the most common methods used to produce microcellular foams is a batch process known as “solid state foaming.” This method was developed in the MIT in the 1980s.<sup>3</sup> It is a two-step method. In the first stage, the polymeric sample is saturated with a non-reactive gas (physical blowing agent) in a pressure vessel. Then, in a second stage, the saturated samples are removed from the pressure vessel and foamed in a temperature-controlled glycerin bath. Finally, the foam is stabilized by cooling.

The field of microcellular foams produced by the solid-state foaming technology has been widely investigated in the last years. Nevertheless, this research has been focused primarily on the foaming of amorphous polymers.<sup>4</sup> The number of investigations in which the microcellular foaming of semi-crystalline polymers is analyzed is lower due to the difficulties found to manufacture microcellular materials with this kind of polymers. The main problems are related to the influence that crystallinity has on the solubility and diffusivity of the blowing agent into the polymer matrix. Particularly, a severe decrease in the solubility and diffusivity takes place due to an increase of the crystallinity.<sup>4-6</sup> As a consequence, obtaining microcellular foams of semi-crystalline polymers is not a simple task. More specifically, the fabrication of high-density polyethylene (HDPE) microcellular materials by solid-state foaming, with low densities is still more complicated due to the quite high crystallinity that this polymer shows (around 60 to 70%). However, in spite of the difficulties, obtaining HDPE microcellular foams is a topic of interest because of the interesting properties of this polymer. HDPE foams are tough, stiff, chemical and abrasion resistant, and present a low absorption and permeability to water and moisture.<sup>7</sup> Moreover, HDPE foams can withstand higher temperatures than low-density polyethylene (LDPE) or ethylene vinyl acetate (EVA) foams, which is an essential requirement for some applications.

Due to the challenges previously mentioned, most of the authors working on this topic have mixed the HDPE with other polymers such as polypropylene (PP)

or with particles with two purposes. The first one consists on improving the bubble nucleation due to the creation of an interface between the immiscible polymers or between the polymer and the particles and the second one consists on decreasing the polymer crystallinity and consequently increasing the gas solubility, that is, the gas concentration available for foaming.<sup>4,5,8–11</sup> As far as the authors know, there are only two works in which a pure HDPE has been successfully foamed with a microcellular structure employing the solid-state foaming process.<sup>6,12</sup> Doroudiani et al.<sup>6</sup> investigated the effect of the crystallinity and the morphology of different semi-crystalline polymers, among them HDPE, on the microcellular processing. They varied the crystallization and morphology of different polymers by subjecting the samples to a compression molding process (at a temperature of 280°C), in which the cooling rate was modified. They obtained the best cellular structures with the samples cooled at the highest rate, in which the lowest crystallinities were achieved. Miller et al.<sup>12</sup> modified the processing conditions (saturation pressure, foaming time and foaming temperature) with the aim of producing low-density HDPE foams with a microcellular structure. They found a processing window effective to produce low-density cellular materials (relative densities of 0.36) with the polymers saturated at a pressure of 3 MPa and foamed at temperatures higher than the melting point.

In this work, blends of HDPE with different amounts of a crosslinking agent have been produced. It is well known that crosslinking has a direct effect on the crystallization process; in general, an increase in the crosslinking degree is related to a decrease in the polymer crystallinity.<sup>13–15</sup> Moreover, as a consequence of crosslinking, the extensional rheological properties of the polymeric matrix in the molten state could be also modified helping to suppress cell coalescence and therefore, increasing the expansion ratio keeping, at the same time, very small cell sizes.<sup>16–19</sup>

The main objective of this work is to perform a thorough study to analyze and understand the foaming mechanisms (nucleation and coalescence) taking place in this particular system with the aim of controlling the foaming process and obtaining cellular materials with low density and improved cellular structures. For this purpose, the foaming time and the foaming temperature have also been modified. The effects that these parameters have on the materials density, cell size, and apparent cell nucleation density have been extensively analyzed.

## Experimental

### Materials

HDPE used in this study is a commercially available grade, Rigidex HD 5211 EA-Y supplied by Ineos Polyolefins with a density of 0.95 g cm<sup>-3</sup> and melt flow rate of 1.1 g min<sup>-1</sup> (190°C, 2.16 kg). An organic peroxide, Luperox 101XLS50 supplied by Arkema was used as crosslinking agent. A commercial grade carbon dioxide (CO<sub>2</sub>) was used as blowing agent.

### Sample preparation

Different blends of HDPE with the crosslinking agent have been prepared by extrusion using a co-rotating twin screw extruder Collin ZK 25T with L/D of 24. The rotational speed was 50 r/min and the melt temperature was 135°C. Three blends of HDPE with different amounts of crosslinking agent (1 pph, 2.4 pph and 4 pph) were produced.

Then, the materials containing the crosslinking agent as well as the pure HDPE were compression molded in a hot plate press. Both pressure and temperature were maintained constant for the different blends, 21.8 bars and 190°C, respectively. The crosslinking time selected for the different formulations was 30 min; however, the sample with the intermediate content of crosslinking agent (2.4 pph) was also crosslinked using times of 15 and 60 minutes. Sheets of 2 mm and 0.5 mm in thickness were produced and these samples were used to manufacture the cellular materials (2 mm in thickness) as well as to perform the extensional rheology measurements (0.5 mm in thickness). The nomenclature used to designate the solid crosslinked HDPE (x-HDPE) materials is as follows:  $C_c-t_c$  where  $C_c$  is the content of crosslinking agent and  $t_c$  is the crosslinking time.

### Gas sorption

HDPE sheets (2 mm in thickness) were cut into 15 mm × 15 mm squares and placed in a pressure vessel. CO<sub>2</sub> gas was introduced at room temperature and samples were allowed to absorb gas. The HDPE samples were saturated at a pressure of 5 MPa.

Samples were periodically removed from the pressure vessel, weighed and returned again to the pressure vessel. With these weight measurements, it was possible to obtain the gas concentration, that is, the weight percentage of CO<sub>2</sub> dissolved in the polymer as a function of the saturation time. The results show that at room temperature (RT) and under a pressure of 5 MPa, 24 hours are necessary to reach the equilibrium gas concentration (gas solubility). The sorption diffusivity coefficient ( $D_s$ ) was also obtained from these measurements using equation (1)

$$\frac{M_s}{M_\infty} = 1 - \frac{8}{\pi^2} \exp\left(\frac{-D_s \pi^2 t_s}{l^2}\right) \quad (1)$$

where  $M_s$  is the sorption amount at time  $t_s$ ,  $M_\infty$  is the saturated sorption amount at a large sorption time and  $l$  is the specimen thickness.<sup>20,21</sup>

### Foaming process

The procedure employed to produce the microcellular foams was the solid-state foaming method.<sup>3,12,22</sup> First, the samples were saturated with CO<sub>2</sub>, as it was described in the previous section, using a saturation pressure of 5 MPa and at

*RT*. During this saturation process, the polymer was always in a solid state. Then, the samples were removed from the pressure vessel and introduced in a temperature-controlled glycerin bath. A thermodynamic instability was created by releasing the pressure and heating the sample causing cell nucleation and growth. Different foaming temperatures (from 150 to 190°C) and different foaming times (from 15 to 75 s) were selected to produce the cellular materials. After foaming, the samples were removed from the glycerin bath and cooled in water at *RT*.

### *Samples characterization*

*Gel content.* The gel content (*GC*) obtained in the HDPE-based polymers after crosslinking was determined according to the ASTM standard D 2765-11. Specimens of the crosslinked ethylene polymers were first weighed and then immersed in xylene which was used as extracting solvent. Samples were kept in boiling xylene during 1.5 h, which is the minimum time necessary to completely dissolve the uncrosslinked HDPE. After this time, the samples were removed from xylene and dried in a vacuum oven pre-heated at 150°C. Finally, the specimens were reweighed to determine the insoluble fraction of polymer and hence, the gel content according to equation (2)

$$GC(\%) = 100 \frac{w_f}{w_0} \quad (2)$$

where  $w_f$  is the weight of the specimen after extraction and drying and  $w_0$  is the weight of the original specimen. Three samples were used to determine the average gel content for each material.

*Differential scanning calorimetry.* Thermal properties of the neat HDPE and the different x-HDPE materials were studied by means of a Mettler DSC822e differential scanning calorimeter, under nitrogen atmosphere, previously calibrated with indium, zinc, and *n*-octane. On the one hand, to obtain the crystallization temperature ( $T_c$ ), the samples were cooled from 200°C to -40°C at 20°C/min. On the other hand, to obtain the crystallinity ( $X_c$ ) and the melting temperature ( $T_m$ ), the samples were heated from -40°C to 200°C at 10°C/min. Before performing these two experiments (cooling and heating), the samples were heated from -40°C to 200°C at a heating rate of 10°C/min and maintained at 200°C during 3 min in order to remove the thermal history of the materials. The crystallinity degree was calculated by dividing the heat of fusion in the DSC curve by the heat of fusion of a 100% crystalline material (288 J/g for a 100% crystalline PE).<sup>23</sup>

*Extensional rheological behavior.* The transient extensional viscosity of the uncrosslinked HDPE as well as that of the x-HDPEs produced with the minimum and

the maximum amounts of peroxide (1 pph and 4 pph) was measured using a stress-controlled rheometer (AR 2000 EX from TA Instruments) with an extensional rheology test fixture (SER 2 from Xpansion Instruments). In this geometry, two clamps hold the sample to two drums, which rotate in opposite direction, stretching the sample at a certain Hencky strain rate.<sup>24</sup>

All the experiments were made at a temperature of 170°C. Rectangular solid samples with dimensions of 20 mm × 10 mm × 0.5 mm fabricated by compression molding, as it was previously described, were used to perform the extensional viscosity measurements.

The measurement protocol considers first a pre-stretch, in order to compensate the thermal expansion of the sample when it is heated up from room temperature. Then, a relaxation step when the pre-stretch has finished. In this step, the sample is kept at the testing temperature (170°C) without applying any stress during 60 s approximately. After this relaxation time, the experiments are performed. Measurements were conducted at three different Hencky strain rates: 0.5, 1 and 2.5 s<sup>-1</sup>. The maximum Hencky strain applied was 2 for all the different materials.

**Density.** Density of the non-foamed (solid), uncrosslinked and crosslinked, polymeric matrices was determined. For this purpose, a gas pycnometer was employed (AccuPyc II 1340 from Micromeritics). The pycnometer provides the volume of the solid samples with high precision as well as the density calculations. Five different measurements of each material were performed with the aim of obtaining and accurate average value of the density of the solid samples.

On the other hand, the density of the cellular materials was determined by the Archimedes water immersion method using a high-precision balance (Mettler AT 261).

Moreover, the relative density of the cellular materials was calculated according to equation (3)

$$\rho_R = \frac{\rho_{cm}}{\rho_s} \quad (3)$$

where  $\rho_{cm}$  is the cellular material density and  $\rho_s$  is the solid matrix density.

**Structural characterization.** Scanning electron microscopy (SEM) was used to analyze the cellular structure. Samples were cooled using liquid nitrogen to cut them without modifying their structure. Then, they were vacuum coated with a thin layer of gold to make them conductive. A Jeol JSM-820 SEM was used to observe the samples morphology.

The micrographs obtained were analyzed with an image processing tool based on the software Fiji/Image J and from these micrographs the following parameters were obtained: the average cell size, the standard deviation of the cell size and the apparent cell nucleation density, which is defined as the number of cells per unit volume of the solid material assuming that coalescence phenomena do not occur

during processing stage. In situations in which cell coalescence occurs during the foaming process (as in this work), the apparent cell nucleation density is useful to compare the overlapping nucleation and coalescence effects. The way in which these parameters are obtained from the SEM micrographs is explained in the work of Pinto et al.<sup>25</sup>

## Results and discussion

### Analysis of solid samples

**Gel content.** HDPE was chemically crosslinked first, by incorporating organic peroxide and then, by activating the peroxide using for this purpose a fixed temperature and different crosslinking times. The crosslinking is randomly produced in the molten state, where the polymer is in an amorphous configuration. In this state, the peroxide links the molecules into a three-dimensional network.<sup>15,26</sup>

Figure 1 shows the gel content which is defined as the fraction of polymer that is insoluble under the test conditions (see Experimental section).

An increase in the gel content is observed when the amount of crosslinking agent increases, while the crosslinking time is kept constant. Furthermore, from Figure 1, it can be derived that the gel content of the crosslinked materials fabricated employing the same content of peroxide is very similar, regardless of the time used to crosslink such materials (that is, for the lowest time used, 15 min, the maximum gel content has already been achieved).

**Thermal characterization.** Table 1 shows the melting temperature, the crystallization temperature and the crystallinity of the uncrosslinked HDPE and the different x-HDPEs. It is well known that crosslinking has a direct effect on the

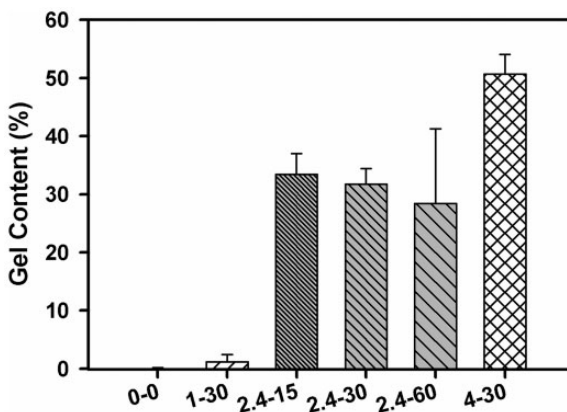


**Figure 1.** Gel content of the uncrosslinked HDPE and the different x-HDPEs.

**Table 1.** Melting temperature ( $T_m$ ), crystallization temperature ( $T_c$ ) and crystallinity ( $X_c$ ) of the neat HDPE and the different crosslinked materials.

Name ( $C_c-t_c$ )	$T_m$ ( $^{\circ}\text{C}$ )	$T_c$ ( $^{\circ}\text{C}$ )	$X_c$ (%)
0-0	129.7	114.2	67.7
1-30	130.0	107.9	62.9
2.4-15	128.9	106.7	60.2
2.4-30	130.1	106.0	57.1
2.4-60	130.5	106.4	58.9
4-30	127.9	107.1	55.8

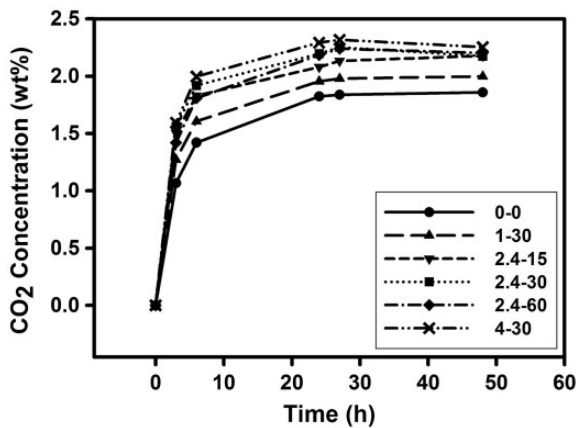


**Figure 2.** Sorption curves of HDPE and x-HDPEs obtained at 5 MPa and room temperature.

crystallization process. Formation of crosslink junctions when the polymer is in a molten state modifies the reorganization and chain folding during the crystallization process. The crosslinks act as defect centers hindering both the crystal growth and the formation of crystals. As a result, imperfect crystallite with smaller sizes and also less in content are formed.<sup>13-15</sup>

The results show that  $T_c$  is lower in the x-HDPEs, although no changes in  $T_c$  are caused by changing the content of the crosslinking agent. Moreover,  $T_m$  remains almost constant and only a slight reduction of this temperature is observed in the material with the highest crosslinking content. However,  $X_c$  decreases significantly with the amount of crosslinking agent. The slight modifications obtained in the thermal properties could be due to the low crosslinking degrees achieved in this work, as the maximum gel content achieved has been just about 50%.

**Diffusivity and gas concentration.** Figure 2 shows the  $\text{CO}_2$  concentration as a function of time of the neat, uncrosslinked, HDPE together with the same curves obtained for the different x-HDPEs.



**Table 2.** Comparison of sorption diffusivity ( $D_s$ ) and gas solubility at equilibrium for the neat HDPE and the different x-HDPE materials.

Name ( $C_c-t_c$ )	$D_s$ ( $10^{-11}$ m <sup>2</sup> /s)	Gas solubility (wt%)
0-0	2.71	1.86
1-30	3.06	1.99
2.4-15	3.44	2.18
2.4-30	3.50	2.18
2.4-60	3.23	2.20
4-30	3.65	2.25

From Figure 2, it can be concluded that both solubility and diffusivity increase with the amount of crosslinking agent (see also Table 2). Moreover, no significant differences are observed between samples with the same amount of crosslinking agent and different crosslinking times, in which the crystallinity was also similar (Table 1) as well as the gel content (Figure 1).

Both diffusivity and solubility of CO<sub>2</sub> in a semi-crystalline sample depend on crystallinity. When crystallinity increases, several aspects that govern the rate of diffusion of the gas molecules into the polymer matrix are modified. On the one hand, an increase in the tortuosity is produced. Small molecules are assumed incapable of diffusing or permeating through the crystalline phase. Therefore, they must pass through a longer path due to the presence of the crystalline phase, which finally leads to a reduction in the diffusion rate. On the other hand, a decrease of the chain segment mobility in the amorphous phase is also produced due to the proximity of crystallites hindering, once again, the diffusion of the gas molecules. Regarding gas solubility, as the gas molecules are only dissolved in the amorphous phase, an increase in the equilibrium gas concentration (solubility) will be produced when the volume of crystalline regions decreases, that is, when the polymer crystallinity decreases.<sup>6,27,28</sup>

Table 2 also indicates that the material with the maximum crosslinking content (4-30) only absorbs 2.25 wt% of gas being, in turn, the polymer that absorbs the highest amount of gas. This low value is indicating that CO<sub>2</sub> has a very low solubility in polyethylene at subcritical pressures and *RT* compared to other polymers like polyvinyl chloride (7.5 wt% at 4.8 MPa and *RT*), polycarbonate (9 wt% at 4.8 MPa and *RT*) and acrylic butadiene styrene (12 wt% at 5 MPa and *RT*).<sup>22,29,30</sup>

Furthermore, the experimental value of the gas concentration achieved for the neat HDPE (1.86 wt% at 5 MPa and *RT*) is in agreement with those reported in literature.<sup>12</sup>

Due to the similar characteristics showed by the three solid crosslinked materials fabricated with the same content of peroxide (2.4 pph) and different crosslinking times, only the material fabricated with a crosslinking time of 30 min has been further studied and foamed.

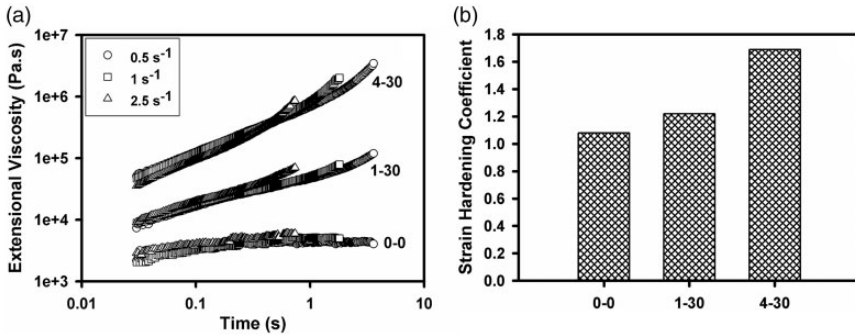


**Figure 3.** Extensinal rheological behavior of the uncrosslinked HDPE (0–0) and the x-HDPEs produced with the minimum (1 phh) and maximum (4 phh) contents of organic peroxide. (a) Extensinal viscosity vs. time measured at different Hencky strain rates: 0.5, 1 and  $2.5 \text{ s}^{-1}$ . (b) Strain hardening coefficient calculated for a time of 2 s and for a Hencky strain rate of  $1 \text{ s}^{-1}$ .

*Extensinal rheological behavior.* During the foaming process, the bubble growth involves extensinal or elongational flow, as the cell walls are stretched. The extensinal viscosity is defined as the ratio between the stress and the strain rate, when a material is elongated. Figure 3(a) shows the transient extensinal viscosity of the uncrosslinked HDPE (0–0) and the x-HDPEs 1–30 and 4–30, measured at three different Hencky strain rates ( $0.5$ ,  $1$  and  $2.5 \text{ s}^{-1}$ ).

When the amount of crosslinking agent increases, an increase in the viscosity of the materials is obtained. Furthermore, while the x-HDPEs show a rapid increase of the extensinal viscosity with time and this behavior become more intense as the amount of crosslinking agent increases, the linear HDPE does not show this behavior. This phenomenon is called strain hardening.<sup>31</sup> In general, if the polymer does not exhibit strain hardening, it is difficult to achieve high expansion ratios during foaming because the cell walls break, that is, cell coalescence is produced and the foam is not able to retain the gas during the expansion process.<sup>32</sup> This strain hardening results from the molecular entanglements in the melt state which can be produced by the introduction of branching or crosslinking.<sup>33,34</sup> With the aim of quantifying this behavior, the strain hardening coefficient ( $S$ ) has been calculated from the extensinal viscosity measurements according to equation (4)

$$S = \frac{\eta_E^+(t, \dot{\epsilon}_0)}{\eta_{E0}^+(t)} \quad (4)$$

where  $\eta_E^+(t, \dot{\epsilon}_0)$  is the transient extensinal viscosity as a function of time and Hencky strain rate and  $\eta_{E0}^+(t)$  is the transient extensinal viscosity in the linear viscoelastic regime.<sup>35,36</sup> The strain hardening coefficient has been obtained for a time of 2 s and for a Hencky strain rate of  $1 \text{ s}^{-1}$ . The results are shown in Figure 3(b). An increase in  $S$  is obtained by increasing the amount of crosslinking

**Table 3.** Summary of the cellular materials produced.

Name ( $C_c-t_c-T_F-t_F$ )	Crosslinking content – $C_c$ (pph)	Crosslinking time – $t_c$ (min)	Foaming temperature – $T_F$ (°C)	Foaming time – $t_F$ (s)
0-0- $T_F-t_F$	0	0	150, 160, 170, 180, 190	15, 30, 45, 75
1-30- $T_F-t_F$	1	30	150, 160, 170, 180, 190	15, 30, 45, 75
2.4-30- $T_F-t_F$	2.4	30	150, 160, 170, 180, 190	15, 30, 45, 75
4-30- $T_F-t_F$	4	30	150, 160, 170, 180, 190	15, 30, 45, 75

agent. In fact, the strain hardening coefficient of the material containing the highest amount of organic peroxide is 1.6 times higher than that of the uncrosslinked HDPE.

Considering the results obtained after the extensional rheological characterization, the x-HDPE containing 4 pph of organic peroxide should be the most suitable material for foaming applications, as it is the material presenting the highest strain hardening coefficient.

### *Analysis of foamed samples*

The most representative solid materials have been foamed as indicated in the Experimental section. All the cellular materials fabricated are summarized in Table 3.

The nomenclature employed to designate the foamed materials is as follows:  $C_c-t_c-T_F-t_F$ , where  $C_c$  is the crosslinking content,  $t_c$  is the crosslinking time,  $T_F$  is the foaming temperature and  $t_F$  is the foaming time.

*Effect of the foaming time.* The effect of the foaming time on the materials density and cellular structure is analyzed in this section. Firstly, the relative density is represented versus the foaming time for the different materials as well as for the following temperatures: 150, 160, 170 and 190°C (Figure 4). In this section, the temperature is also considered with the aim of determining if the behaviors obtained when the density is represented as a function of time are also dependent on the foaming temperature.

The results indicate that the minimum relative density (0.37) has been achieved using the polymer containing the highest amount of peroxide (4 pph) and with the following foaming conditions: a foaming time of 30 s and a foaming temperature of 160°C.

With the exception of the cellular materials fabricated with the highest foaming temperature (190°C) in which the relative density increases with time, for the rest of materials the relative density shows a minimum for a foaming time of approximately 30 s. If the foaming time is not high enough, the materials do not foam completely and only the surface is expanded; as a consequence, only a small

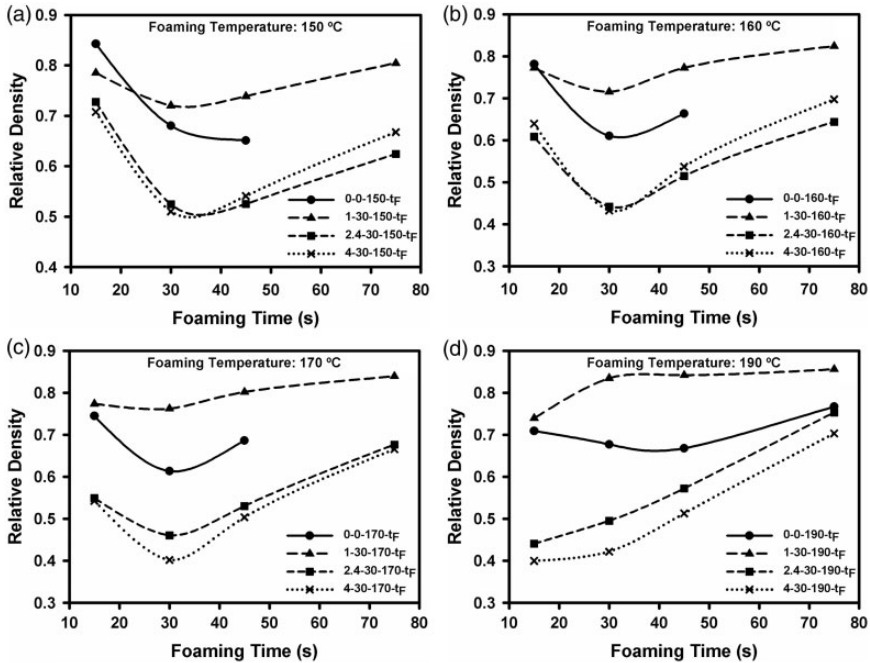


**Figure 4.** Relative densities of the different materials as a function of the foaming time for the different foaming temperatures. (a) 150°C, (b) 160°C, (c) 170°C and (d) 190°C.

reduction in density is obtained. When the foaming time increases from 15 to 30 s, a significant reduction in density is observed. This time allows producing a large expansion of the polymeric material. Then, when the foaming time increases again, an increase in density is produced. The gas is continuously diffusing out of the material and therefore, if the structure is not frozen in an optimum time, the cells begin to collapse causing foam contraction. Moreover, when the foaming time increases, cell coalescence also occurs. These two phenomena make the density to increase if the foaming time is too high. Nevertheless, this behavior is not followed by the cellular materials manufactured with the highest foaming temperature (190°C). In this particular case, the relative density always increases with the foaming time. This temperature is very high and consequently the gas diffusion and the coalescence mechanisms are favored. The minimum in density is not observed because this minimum would appear at lower times than those studied in this work, that is, a similar behavior than that obtained with the other temperatures could be obtained if lower foaming times were considered.

Taking into account the previous results, the effect of the foaming time on the cellular structure has been studied considering only a representative temperature (160°C). Moreover, this study has been performed in the two most extreme

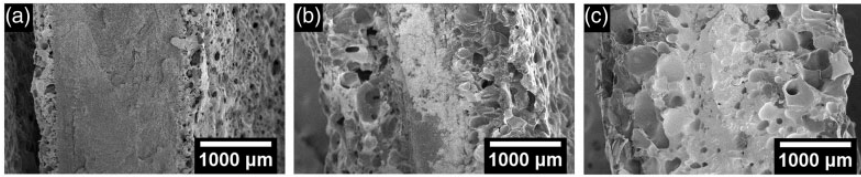


**Figure 5.** SEM micrographs of the cellular materials fabricated with the uncrosslinked HDPE, with a foaming temperature of 160°C and different foaming times. (a) 15 s, (b) 30 s and (c) 45 s.

materials: the uncrosslinked HDPE and the material produced with the x-HDPE containing the highest amount of peroxide.

The cellular structure of the materials fabricated with the uncrosslinked HDPE (0-0) at different foaming times is shown in Figure 5.

Only the surface of these materials is foamed. The differences obtained in density could be related perfectly with those found in the cellular structures of the different foamed materials. When a foaming time of 15 s is employed, almost all the material is still solid and only a very narrow band of the surface is foamed. Therefore, the reduction of density obtained in this material is very low. For a higher foaming time (30 s), a significant reduction in density is obtained. SEM micrograph of this material shows that the foamed band is wider than in the previous material. Finally, for the highest foaming time (45 s), an increase in the density is again produced. The width of the foamed band is similar to that of the previous material but larger cells appear on the surface which indicates that cell coalescence and hence, foam collapse have been produced making the overall density to increase.

In the same way, the cellular structure of the foamed materials fabricated with the x-HDPE containing 4 pph of crosslinking agent has been analyzed. The SEM micrographs are shown in Figure 6. In this case, most of the samples are completely foamed and therefore, the micrographs have been taken from the center of the sample in order to compare the cellular structure under the same conditions. Figure 6 shows the most representative structures of each material.

Apart from the material manufactured with the lowest foaming time (15 s), the rest of materials are completely foamed, that is, both the surface and the center are expanded.

In order to analyze more accurately the cellular structure of the foamed materials both, the cell size and the apparent cell nucleation density have been quantified. In the samples completely foamed, the image analysis was performed in the center of the sample; however, the whole fractured section, including both the center and the sides close to the foamed surface (see Figure 5), was considered in the non-completely foamed samples. The results obtained for the two materials are shown in Figure 7.

The average cell size (Figure 7(a)) of the foamed materials produced with the x-HDPE (4 pph) does not change with the foaming time; however, an increase of this parameter is produced when the material foamed is the uncrosslinked HDPE.

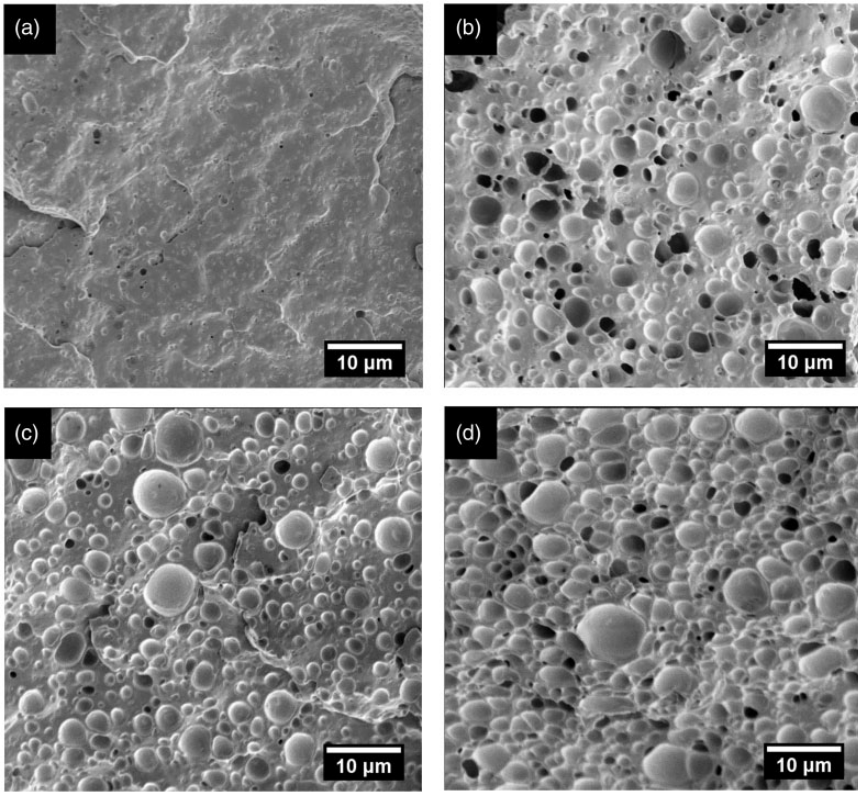


**Figure 6.** SEM micrographs of the cellular materials fabricated with the x-HDPE, containing 4 pph of organic peroxide, with a foaming temperature of 160°C and with different foaming times. (a) 15 s, (b) 30 s, (c) 45 s and (d) 75 s.

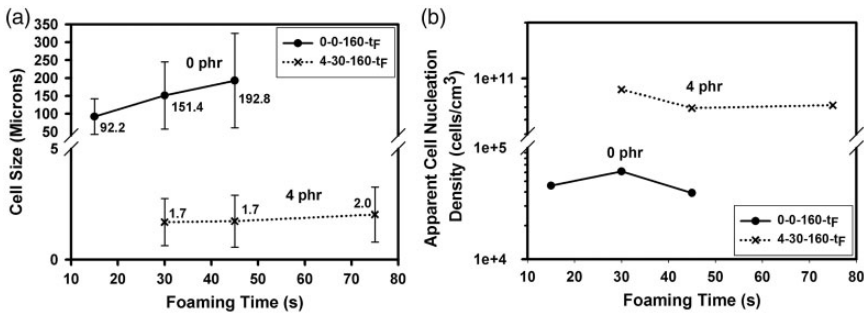


**Figure 7.** Effect of the foaming time on the cellular structure in both the foamed uncrosslinked HDPE and the foamed x-HDPE containing 4 pph of crosslinking agent. (a) Cell size as a function of the foaming time and (b) apparent cell nucleation density vs. foaming time.

The cell size is doubled by going from 15 to 45 s. Another important fact is that the average cell size of the foamed uncrosslinked HDPE materials is two orders of magnitude higher than that of the cellular materials produced with the x-HDPE. This behavior could be explained taking into account that the strain hardening is larger in the crosslinked materials (Figure 3), which could lead to a less intense coalescence phenomenon and hence to cells with smaller sizes. Moreover, solubility results indicate that the amount of gas available for foaming is slightly higher in the crosslinked materials. As a consequence, the number of homogeneous nucleation sites could be also greater in this material leading to smaller cell sizes.<sup>37</sup>

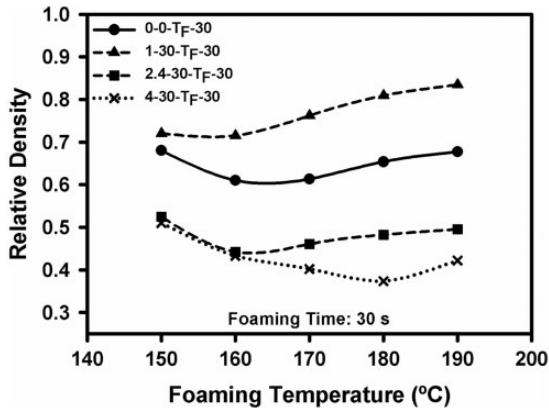
In the two types of materials, the standard deviation of the cell size is really high, which indicates that the cellular structures are very heterogeneous.

Figure 7(b) shows the apparent cell nucleation density versus the foaming time. This parameter allows comparing materials with different densities, as this parameter takes into account the relative density of the foamed materials.<sup>25</sup> Therefore, with this parameter it is possible to analyze both, nucleation and coalescence mechanisms. In general, when the foaming times are low, nucleation is the predominant phenomenon. Then, when the foaming time increases, cell coalescence also takes place. In the material produced with the uncrosslinked HDPE, an increase in the apparent cell nucleation density is obtained when the foaming time increases from 15 to 30 s. This fact indicates that new cells have appeared. Although cell coalescence could be also happening, in these foaming times, the nucleation phenomenon prevails over the coalescence one. Then, when the foaming time increases from 30 to 45 s, cell coalescence is the predominant phenomenon making the apparent cell nucleation density to decrease. In the cellular materials based on the x-HDPE,  $N_V$  remains almost constant. This behavior can be explained taking into account the rheological results represented in Figure 3. The strain hardening exhibited by the x-HDPE helps to stabilize the cellular structure.

**Effect of the foaming temperature.** In this section, the effect of the foaming temperature on the relative density and cellular structure of the different materials is studied. To perform this analysis, a foaming time of 30 s has been selected as, in general, with this foaming time the lowest densities are achieved (see Figure 4). In Figure 8, the relative density of the different foamed materials is represented versus the foaming temperature.

When the foaming temperature increases, the viscosity of the polymeric materials decreases and therefore, the initial growth of the cells is favored. This greater cell growth could result in a reduction of the materials density. Moreover, the classical nucleation theory (equation (5)) states that the homogeneous nucleation rate ( $N_{HOM}$ ) also increases with temperature, which also would contribute to reduce the foams density<sup>38</sup>

$$N_{HOM} = C_0 f_0 \exp\left(\frac{-\Delta G^*}{kT}\right) \quad (5)$$



**Figure 8.** Relative densities of the different materials produced using a foaming time of 30 s, as a function of the foaming temperature.

where  $C_0$  is the concentration of gas molecules,  $f_0$  is the frequency factor of the gas molecules,  $\Delta G^*$  is the activation energy,  $k$  is the Boltzman's constant and  $T$  is the temperature.

However, the fact of increasing the foaming temperature has also some disadvantages. When the temperature increases, the chain mobility increases and therefore, the diffusion rate also increases.<sup>39</sup> The blowing agent that has diffused into the nucleated cells would tend to diffuse out of the material. If the gas escapes through the cell walls, the amount of gas available for the cell growth would decrease. As a result, if the cells do not freeze, they would tend to collapse causing foam contraction and therefore, increasing the materials density.<sup>40</sup> Moreover, an increase in the foaming temperature is also related to an increase in the cell coalescence, as the polymer melt strength decreases when the temperature increases.<sup>41</sup> As a consequence, the overall density of the material would also increase.

Figure 8 indicates that the behavior followed by all the materials is the same. When the temperature increases first, the relative density decreases and then, this parameter increases. When the foaming temperatures are low enough, the polymer is capable of resisting the extension without breaking and therefore an increase in the foaming temperature leads to a reduction in density because the cell growth and the cell nucleation rate are favored, as it was previously explained. However, when the temperatures are higher, the gas escapes more easily and the polymeric matrix is not able to resist the extension (since the melt strength decreases as the temperature increases). As a consequence, both cell coalescence and foam collapse prevail over cell nucleation and cell growth, giving as a result an increase in the foams density.

Changes in the cellular structure by varying the foaming temperature are analyzed once again in the two extreme materials: the uncrosslinked HDPE (0-0) and the x-HDPE containing the highest amount of organic peroxide. To perform



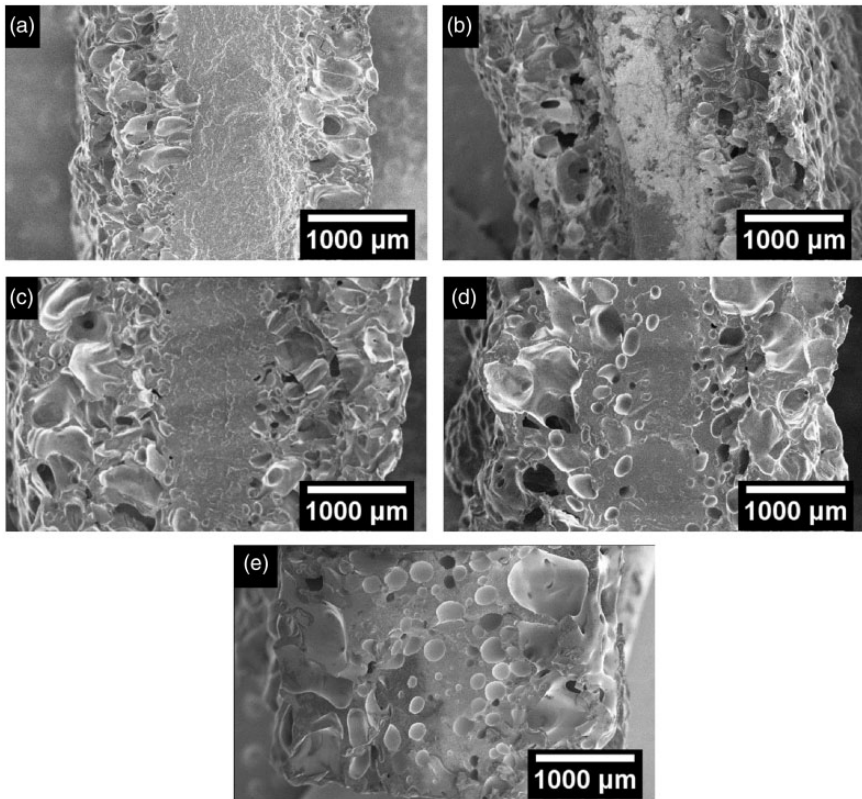


**Figure 9.** SEM micrographs of the cellular materials fabricated with the uncrosslinked HDPE, with a foaming time of 30 s and with different foaming temperatures. (a) 150°C, (b) 160°C, (c) 170°C, (d) 180°C and (e) 190°C.

this analysis, the foaming time considered for both materials is once again 30 s. Figure 9 shows the complete area of the cellular materials fabricated with the uncrosslinked HDPE for the different foaming temperatures analyzed.

In general, the center of these foamed materials is mostly solid, whereas the surface is foamed. Nevertheless, it can be seen that when the temperature increases some isolated pores begin to appear in the center. Moreover, it can be appreciated that larger cells in the surface are also obtained by increasing the foaming temperature. The surface cells are the first to be formed; therefore, if the foaming temperature is very high, cell coalescence is produced in the surface and consequently, an increase in the foams density occurs.

In the same way, the cellular structure of the foamed x-HDPEs containing 4 pph of crosslinking agent and fabricated with different foaming temperatures has been carefully analyzed. Figure 10 shows the SEM micrographs of the different materials. In this case, most of the samples are completely foamed. The micrographs

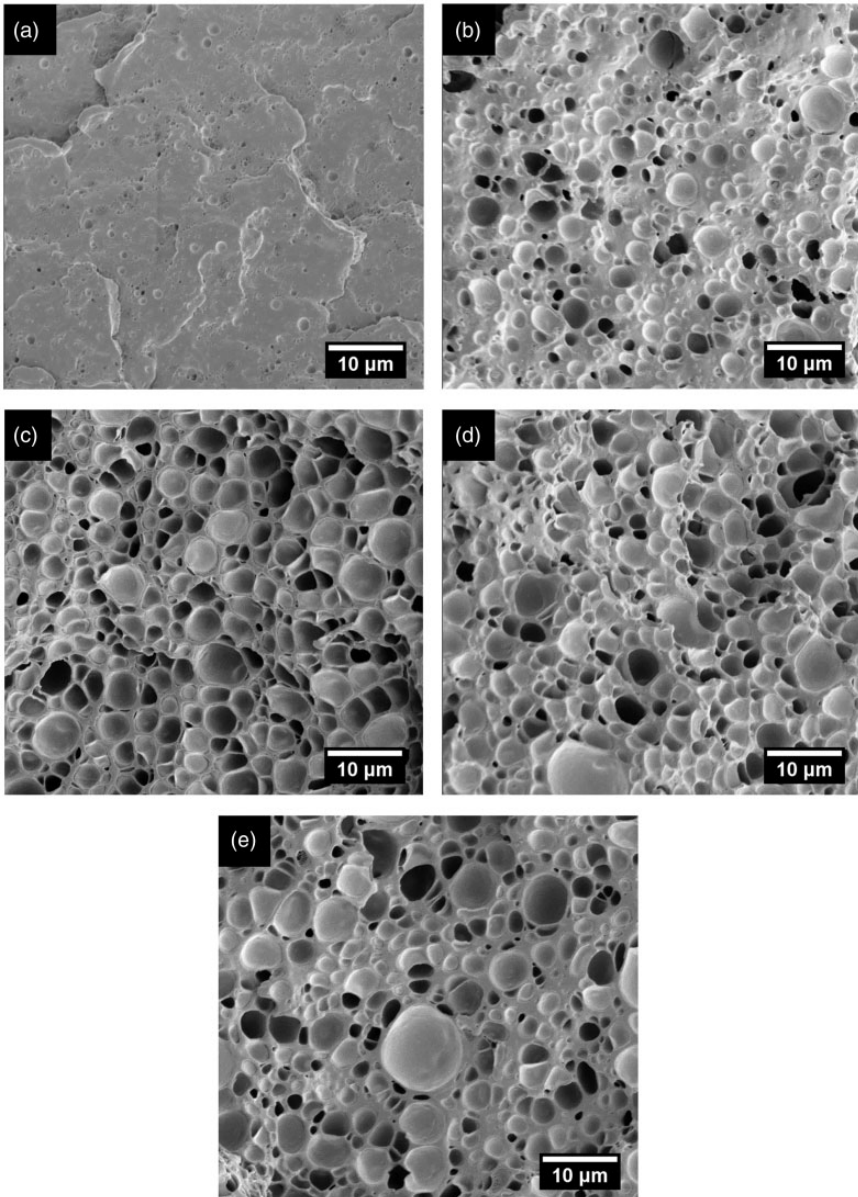


**Figure 10.** SEM micrographs of the cellular materials fabricated with the x-HDPE, containing the highest amount of organic peroxide (4 phh), with a foaming time of 30 s and different foaming temperatures. (a) 150°C, (b) 160°C, (c) 170°C, (d) 180°C and (e) 190°C.

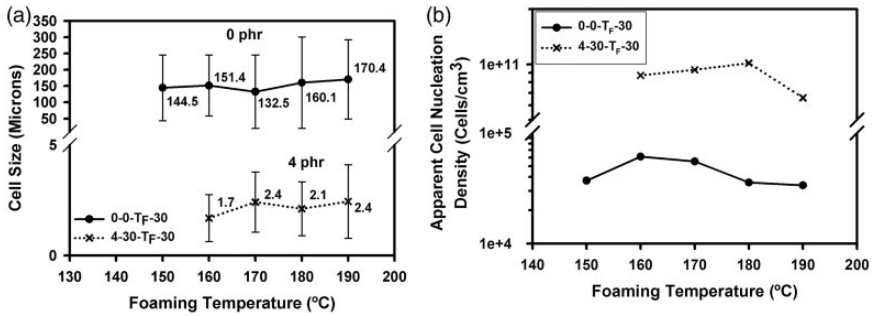


**Figure 11.** Effect of the foaming temperature on the cellular structure in both the foamed uncrosslinked HDPE and the foamed x-HDPE containing 4 pph of crosslinking agent. (a) Cell size as a function of the foaming time. (b) Apparent cell nucleation density vs. foaming time.

have been taken from the center of the sample in order to compare the cellular structure under the same conditions.

The center of the material produced employing the lowest foaming temperature (150°C) is not foamed, and consequently, the global relative density of this material is the highest one.

In order to analyze more accurately the cellular structure of the foamed materials, the average cell size and the apparent cell nucleation density have been quantified. The image analysis was performed in the same regions as those employed in the analysis of the effects produced by changing the foaming time. Both parameters are represented as a function of temperature in Figure 11.

In general, a slight increase in the cell size is detected by changing the foaming temperature. Furthermore, the cell size standard deviation is again really high, independently on the foaming temperature, which gives an idea of the heterogeneity of the cellular structures. To analyze the mechanisms taking place during the foaming process, the behavior of the apparent cell nucleation density is analyzed. In the cellular materials produced with the uncrosslinked HDPE, the apparent cell nucleation density increases when the temperature goes from 150 to 160°C. Moreover, in this range of temperature also a reduction of the relative density was detected (Figure 8). This indicates that, in this temperature range, cell coalescence has not yet occurred, as it was previously concluded. The increase on the temperature is favoring the nucleation rate, and consequently, the apparent cell nucleation density increases. Then, when the temperature raises again the apparent cell nucleation density decreases, indicating that cell coalescence is now one of the prevailing mechanisms. In the foamed x-HDPE, a similar behavior is detected. However, the coalescence phenomenon begins to occur at higher temperatures (180°C). The large strain hardening of this materials helps to stabilize their cellular structure. Therefore, higher temperatures are required to produce a degeneration of the mentioned cellular structure.

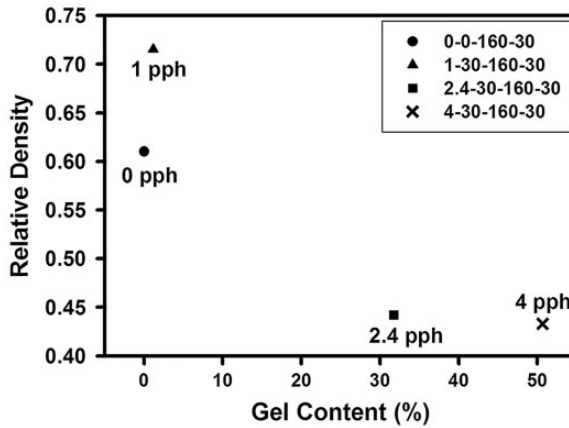


**Figure 12.** Relative density as a function of the gel content for the cellular materials fabricated with a foaming time of 30 s and a foaming temperature of 160°C.

*Effect of the crosslinking content.* Throughout the previous sections, important differences have been found between the two extreme materials: the uncrosslinked HDPE and the x-HDPE with the highest content of peroxide. These different behaviors indicate that the effect of the crosslinking degree on the foam density and cellular structure should be analyzed in detail. For this purpose, the relative density is represented as a function of the gel content (Figure 12). Both, the foaming time and the foaming temperature have been kept constant. A foaming time of 30 s and a foaming temperature of 160°C have been considered.

In general, when the crosslinking degree increases, the relative density decreases. As it was previously shown, the strain hardening increases with the amount of crosslinking agent (Figure 3); therefore, higher expansion ratios can be achieved due to the ability of the foam to retain the gas during the foaming process. Moreover, the gas solubility also increases with the crosslinking degree (Table 2). As a result of this slight increase of the amount of gas available for foaming, cellular materials with higher expansion ratios and therefore, with lower relative densities can be obtained.

On the other hand, the microcellular material fabricated with a content of peroxide of 1 pph does not follow this trend. The gas solubility in this material is higher than in the uncrosslinked HDPE but its relative density is also higher. When a polymer is crosslinked, its viscosity is enhanced to a very high value, as it was indicated in Figure 3. Therefore, the viscosity of the polymer 1–30 is higher than that of the uncrosslinked HDPE. Moreover, the gas concentration of this material is lower than the gas concentration of the other x-HDPEs. This increment in the viscosity together with a not very high amount of gas available for foaming hinders the growth of cells. As a consequence, the cellular materials fabricated with this polymer exhibit the highest densities.

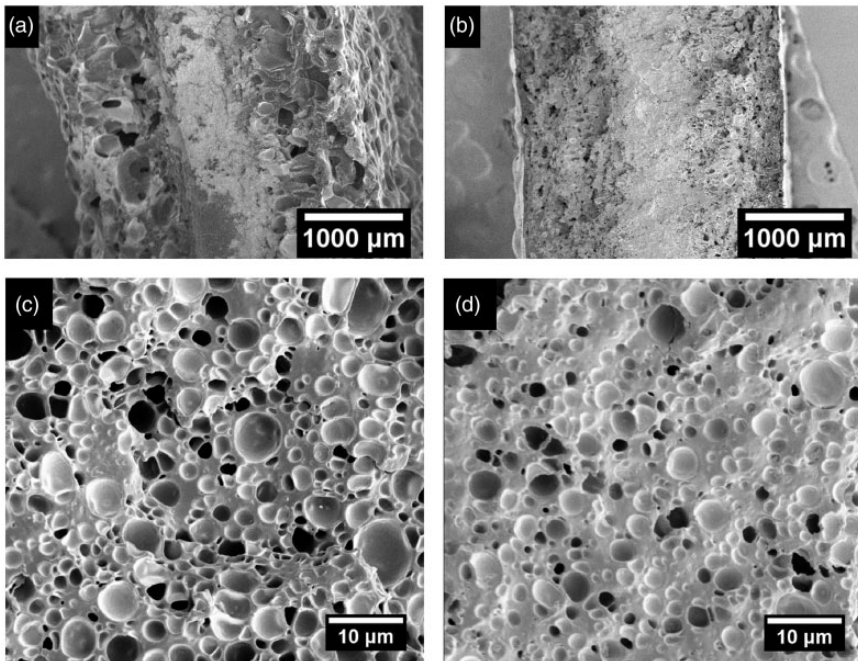


**Figure 13.** SEM micrographs of the cellular materials fabricated employing different x-HDPE, (a) 0-0-160-30, (b) 1-30-160-30, (c) 2.4-30-160-30 and (d) 4-30-160-30.

SEM micrographs of the four cellular materials studied in this section are shown in Figure 13.

Figure 13(a) and (b) shows the complete area of the cellular materials produced with the polymers containing the lowest amounts of crosslinking agent (0 pph and 1 pph). In these micrographs, it is possible to see a non-homogenous foaming. The surface of both materials is completely foamed; however, while the center of the material containing the lowest amount of peroxide is completely solid, a small number of pores appear on the material containing 1 pph of organic peroxide. Nevertheless, with the x-HDPEs containing higher contents of peroxide (2.4 pph and 4 pph), a complete expansion is obtained. The amount of gas available is now large enough to allow a complete expansion of the whole material. As both the center and the surface are completely foamed, greater reductions in density are obtained in these materials. In this case, to illustrate the cellular structure in more detail, the micrographs show a central region of the foamed materials (Figure 13(c) and (d)).

To have further details of how the cellular structure is affected by increasing the amount of crosslinking content, the average cell size and the apparent cell nucleation density have been quantified. The results obtained are represented as a function of the gel content in Figure 14.

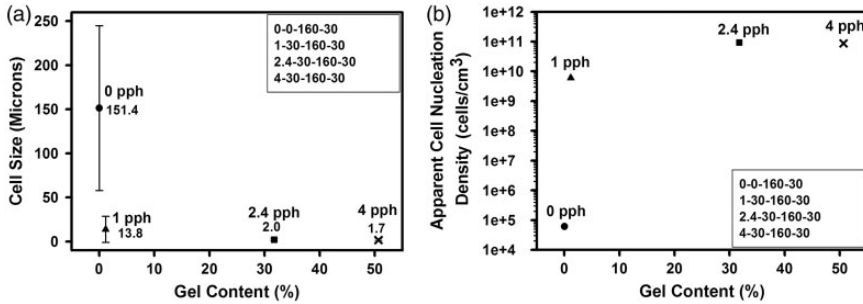


**Figure 14.** Effect of the crosslinking content on the cellular structure. (a) Cell size as a function of the gel content. (b) Apparent cell nucleation density vs. gel content.

In general, when the gel content increases, a reduction in the cell size and an increase in the apparent cell nucleation density is observed. In this case, the cellular materials are produced using the same foaming parameters and therefore, the changes obtained in the cellular structure can be explained taking into account, on the one hand, the rheological properties of the polymeric matrices and, on the other hand, the amount of gas available for foaming. When the gel content increases the strain hardening also increases. Consequently, the cell walls are more resistant to the extension and the cell coalescence decreases. As a result, cellular structures with lower cell sizes and higher apparent cell nucleation densities are obtained. On the other hand, the gas solubility increases slightly as the gel content increases. Therefore, an increase in the number of nucleation sites is also produced. Consequently, both the surface and the center expand and the apparent cell nucleation density increases. Furthermore, an increase in the number of nucleation sites also leads to a reduction in the cell size.

As expected, the best results are obtained with the polymer with the highest crosslinking degree because of its greater ability to absorb CO<sub>2</sub> and its improved rheological properties.

## Conclusions

In this work, the effects that the foaming time, the foaming temperature and the crosslinking content have on the density and microcellular structure of  $\alpha$ -HDPE based foamed materials have been analyzed, with the aim of understanding the mechanisms taking place during the foaming process. First, the solid materials were studied. When the amount of crosslinking agent increases, the strain hardening coefficient increases as well as the gel content. Moreover, a reduction in the crystallinity is also observed with the consequent increase of the gas solubility (and hence, of the amount of gas available for foaming). Then, the effect of the foaming time is examined. A minimum in density has been obtained by changing the foaming time. Moreover, it is found that the structure of the foams produced with the  $\alpha$ -HDPE containing the highest amount of peroxide is very stable. No changes are

detected neither in the cell size nor in the apparent cell nucleation density, due to the high strain hardening that this material shows. The effect of the foaming temperature has also been carefully analyzed. As with the foaming time, a minimum in the relative density was obtained by changing the foaming temperature. In this case, the apparent cell nucleation density shows a maximum independently on the material used to produce the cellular materials. Moreover, the maximum in the apparent cell nucleation density of the material with the highest crosslinking degree is produced at higher temperatures than that of the uncrosslinked HDPE, due to its favorable rheological properties. Finally, the effect of the crosslinking content has been analyzed. While the relative density and the cell size decrease with the gel content, an increase in the apparent cell nucleation density is obtained. This behavior has been explained considering, on the one hand, the improvements achieved in the extensional rheological behavior by increasing the gel content and, on the other hand, the increase in the amount of gas available for foaming.

To conclude, the results indicate that cellular materials with relative densities as low as 0.37 and with cell sizes of approximately  $2\ \mu\text{m}$  can be produced using a saturation pressure of 5 MPa, a foaming time of 30 s, a foaming temperature of  $160^\circ\text{C}$  and a crosslinked HDPE with a gel content of 50%. There is a clear relationship between the extensional rheological behaviors of the solid polymeric matrices and the cellular structure of the foams. By crosslinking the polymeric matrix, it is possible to obtain foamed materials with an improved cellular structure compared to that obtained with the uncrosslinked polymer.

### Declaration of conflicting interests

The author(s) declared no potential conflicts of interest with respect to the research, authorship, and/or publication of this article.

### Funding

Financial support from PIRTU contract of E. Laguna-Gutierrez by Junta of Castile and Leon (EDU/289/2011) and co-financed by the European Social Fund is gratefully acknowledged. Financial assistance from MINECO and FEDER program (MAT 2012-34901), MINECO, FEDER, European Union (EU) (MAT2015-69234-R) and the Junta de Castile and Leon (VA035U13) are gratefully acknowledged.

### References

1. Park CB. Continuous production of high-density and low-density microcellular plastics in extrusion. In: Lee ST (ed.) *Foam extrusion: principles and practice*, 1st ed. Lancaster: Technomic Publishing Company Inc., 2000, pp.274–316.
2. Kumar V. Microcellular polymers. Novel materials for the 21st-century. *Cell Polym* 1993; 12: 207–223.
3. Martini-Vvedensky JE, Suh NP and Waldman FA. *Microcellular closed cell foams and their method of manufacture*. Patent 4473665-A, USA, 1984.
4. Rachtanapun P, Selke SEM and Matuana LM. Microcellular foam of polymer blends of HDPE/PP and their composites with wood fiber. *J Appl Polym Sci* 2003; 88: 2842–2850.

5. Doroudiani S, Park CB and Kortschot MT. Processing and characterization of microcellular foamed high-density polyethylene/isotactic polypropylene blends. *Polym Eng Sci* 1998; 38: 1205–1215.
6. Doroudiani S, Park CB and Kortschot MT. Effect of the crystallinity and morphology on the microcellular foam structure of semicrystalline polymers. *Polym Eng Sci* 1996; 21: 2645–2662.
7. Biron M. Detailed accounts of thermoplastics resins. In: Biron M (ed.) *Thermoplastics and thermoplastic composites: technical information for plastics users*, 1st ed. Oxford: Butterworth-Heinemann, 2007, pp.217–715.
8. Rachtanapun P, Selke SEM and Matuana LM. Relationship between cell morphology and impact strength of microcellular foamed high-density polyethylene/polypropylene blends. *Polym Eng Sci* 2004; 8: 1551–1560.
9. Rachtanapun P, Selke SEM and Matuana LM. Effect of the high-density polyethylene melt index on the microcellular foaming of high-density polyethylene/polypropylene blends. *J Appl Polym Sci* 2004; 93: 364–371.
10. Lee YH, Park CB, Wang KH, et al. HDPE-clay nanocomposite foams blown with supercritical CO<sub>2</sub>. *J Cell Plast* 2005; 41: 487–502.
11. Jo C and Naguib HE. Constitutive modeling of HDPE polymer/clay nanocomposite foams. *Polymer* 2007; 48: 3349–3360.
12. Miller D and Kumar V. Fabrication of microcellular HDPE foams in a sub-critical CO<sub>2</sub> process. *Cell Polym* 2009; 28: 25–40.
13. Khonakdar HA, Morshedean J, Wagenknecht U, et al. An investigation of chemical cross-linking effect on properties of high-density polyethylene. *Polymer* 2003; 44: 4301–4309.
14. Khonakdar HA, Morshedean J, Mehrabzadeh M, et al. Thermal and shrinkage behaviour of stretched peroxide-crosslinked high-density polyethylene. *Eur Polym J* 2003; 39: 1729–1734.
15. Khonakdar HA, Jafari SH, Taheri M, et al. Thermal and wide angle X-ray analysis of chemically and radiation-crosslinked low and high density polyethylenes. *J Appl Polym Sci* 2006; 100: 3264–3271.
16. Nam GJ, Yoo JH and Lee JW. Effect of long-chain branches of polypropylene on rheological properties and foam-extrusion performances. *J Appl Polym Sci* 2005; 96: 1793–1800.
17. Spitael P and Macoko CW. Strain hardening in polypropylenes and its role in extrusion foaming. *Polym Eng Sci* 2004; 44: 2090–2100.
18. Stange J and Müntstedt H. Effect of long-chain branching on the foaming of polypropylene with azodicarbonamide. *J Cell Plast* 2006; 42: 445–467.
19. Yamaguchi M and Suzuki K. Rheological properties and foam processability for blends of linear and crosslinked polyethylenes. *J Polym Sci Pol Phys* 2001; 39: 2159–2167.
20. Tang M, Du TB and Chen YP. Sorption and diffusion of supercritical carbon dioxide in polycarbonate. *J Supercrit Fluid* 2004; 28: 207–218.
21. Nawaby AW and Zhang ZR. Solubility and diffusivity. In: Gendron R (ed.) *Thermoplastic foam processing. Principles and development*, 1st ed. Boca Raton: CRC Press, 2004, pp.1–42.
22. Kumar V and Weller JE. A process to produce microcellular PVC. *Int Polym Proc* 1993; 8: 73–80.
23. Peacock AJ. *Handbook of polyethylene: structure, properties and applications*. New York: Marcel Dekker, Inc., 2000, p.177.



24. Sentmanat M and McKinley GH. Measuring the transient extensional rheology of polyethylene melts using the SER universal testing platform. *J Rheol* 2005; 49: 585–606.
25. Pinto J, Solorzano E, Rodriguez-Perez MA, et al. Characterization of the cellular structure based on user-interactive image analysis procedures. *J Cell Plast* 2013; 49: 555–575.
26. Tamboli SM, Mhaske ST and Kale DD. Crosslinked polyethylene. *Indian J Chem Tech* 2004; 11: 853–864.
27. Michaels AS and Bixler HJ. Solubility of gases in polyethylene. *J Polym Sci Pol Chem* 1961; 50: 393–412.
28. Kanehashi S, Kusakabe A, Sato S, et al. Analysis of permeability; solubility and diffusivity of carbon dioxide; oxygen; and nitrogen in crystalline and liquid crystalline polymers. *J Membrane Sci* 2010; 365: 40–51.
29. Kumar V and Weller J. production of microcellular polycarbonate using carbon-dioxide for bubble nucleation. *J Eng Ind-T ASME* 1994; 116: 413–420.
30. Murray RE, Weller JE and Kumar V. Solid-state microcellular acrylonitrile-butadiene-styrene foams. *Cell Polym* 2000; 16: 413–425.
31. Gendron R and Daigneault LE. Rheology of thermoplastic foam extrusion process. In: Lee ST (ed.) *Foam extrusion: principles and practice*, 1st ed. Lancaster: Technomic Publishing Company Inc., 2000, pp.35–80.
32. Naguib HE, Park CB, Panzer U, et al. Strategies for achieving ultra low-density polypropylene foams. *Polym Eng Sci* 2002; 42: 1481–1492.
33. Lugao AB, Artel BWH, Yoshiga A, et al. Production of high melt strength polypropylene by gamma irradiation. *Radiat Phys Chem* 2007; 76: 1691–1695.
34. Sugimoto M, Tanaka T, Masabuchi Y, et al. Effect of chain structure on the melt rheology of modified polypropylene. *J Appl Polym Sci* 1999; 73: 1493–1500.
35. Stange J, Uhl C and Münstedt H. Rheological behavior of blends from a linear and a long-chain branched polypropylene. *J Rheol* 2005; 49: 1059–1079.
36. Chaudhary AK and Jayaraman K. Extrusion of linear polypropylene–clay nanocomposite foams. *Polym Eng Sci* 2011; 51: 1749–1756.
37. Kumar V and Weller JE. A model for the unfoamed skin on microcellular foams. *Polym Eng Sci* 1994; 34: 169–173.
38. Colton J and Shu NP. Nucleation of microcellular foam. Theory and practice. *Polym Eng Sci* 1987; 27: 500–503.
39. George SC and Thomas S. Transport phenomena through polymeric systems. *Prog Polym Sci* 2001; 26: 985–1017.
40. Park CB, Behraves AH and Venter RD. Low density microcellular foam processing in extrusion using CO<sub>2</sub>. *Polym Eng Sci* 1998; 38: 1812–1823.
41. Wagner MH. Elongational viscosity and its meaning for the praxis. In: Karger-Kocsis J (ed.) *Polypropylene an A-Z reference*, 1st ed. New York: Springer Science + Bussines Media, 1999, pp.198–205.